Journal of Solid State Chemistry 181 (2008) 1220–1226

Contents lists available at ScienceDirect

Journal of Solid State Chemistry

journal homepage: www.elsevier.com/locate/jssc

Impact of metal substitutions for cobalt in $YBaCo_4O_7$

A. Maignan *, V. Caignaert, V. Pralong, D. Pelloquin, S. Hébert

Laboratoire CRISMAT, UMR 6508 CNRS ENSICAEN, 6 bd du Maréchal Juin, 14050 CAEN Cedex 4, France

ARTICLE INFO

Article history:
Received 5 December 2007
Received in revised form
6 February 2008
Accepted 13 February 2008
Available online 4 March 2008

Keywords:
Oxide
Cobaltite
Metal–insulator transition
Structural transition

ABSTRACT

The "114" $YBaCo_4O_7$ cobaltite undergoes structural transition just beyond room temperature at T_S~310 K. Correspondingly, its signature in the physical properties is detected by T-dependent measurements of electrical resistivity, magnetic susceptibility and thermoelectric power. It is found that low-level substitutions of divalent ($M = Zn^{2+}$) or trivalent ($M = Ga^{3+}$, Al^{3+}) cations for cobalt according to the $YBaCo_{4-x}M_xO_7$ formula with $x \leqslant 0.4$ have a strong impact upon this transition. On the one hand, Zn^{2+} substitutions preserve the transition but with T_S decreasing as x increases. On the other hand, for $x = 0.2$ Ga^{3+} or Al^{3+}, the transition is suppressed, i.e., for only 5% trivalent foreign cation substituted for cobalt. Though at first, this contrasted behaviour between divalent and trivalent substituting cations appears to be linked to the opposite evolution of hole carriers "Co^{3+}" concentration with x, a possible destabilization of $3Co^{2+}$: $1Co^{3+}$ charge ordering induced by the M^{3+} cations is considered.

1. Introduction

Recently, the coupled electronic and magnetic structural transition at T_S in the compounds $LBaCo_4O_7$ [L = lanthanide (or Y^{3+}) such as $r_L \leqslant r_{Tb3+}$] has attracted much attention [1–12]. In particular, the T_S dependence on the L^{3+} ionic radius [7,9] has not been explained in this structure containing $Co^{2+/3+}O_4$ tetrahedra with cobalt ions forming Kagomé layers [Co(2)] alternating with adjacent triangular layers [Co(1)] (Fig. 1). For $L = Y^{3+}$, this strongly frustrated spins system orders antiferromagnetically below T_N~105 K, whereas for $T_N \leqslant T < T_S$ (~310 K) only diffuse magnetic scattering occurs [4]. Above T_S the low T orthorhombic ($Pbn2_1$) structure transforms to trigonal symmetry ($P31c$), the latter being paramagnetic and more conducting [4]. Thermoelectric power measurements also confirm the change of electronic conduction at T_S with hole (Co^{3+}) localization in the Co^{2+} matrix as the local magnetic coupling becomes antiferromagnetic for $T < T_S$ [6]. However, since the 1:3 ratio of Co^{3+}/Co^{2+} from the chemical formula corresponds exactly to the ratio of cobalt crystallographic sites, one Co(1) site in the triangular sheet for three Co(2) sites in the Kagomé layer (Fig. 1), and despite the lack of evidence coming from neutron diffraction, one might consider the existence of Co^{2+}/Co^{3+} orbital, charge, spin ordering to explain the observed change at T_S.

For the solid-state chemist, the study of site selective chemical substitutions could give important information about the origin of the transition. For this purpose, three cations with d^0 or d^{10} electronic configurations ($M = Al^{3+}$, Ga^{3+} and Zn^{2+}) have been selected for their strong affinity towards the fourfold coordination of MO_4 tetrahedron. In previous studies, it was shown that: (i) up to three Zn^{2+} can be substituted over the four cobalt cations of $YBaCo_4O_7$ strongly suggesting that all the Co(2) crystallographic sites of the Kagomé layer can be substituted by Zn^{2+} [13], (ii) the Al^{3+} solubility appears to be very limited but can be extended to one Al^{3+} as in $CaBaFeZn_2AlO_7$ [5] and $CaBaCo_3AlO_7$ [14] which suggests a greater Al^{3+} affinity for the Co(1) crystallographic site of the triangular plane. To our knowledge, there exists no report about the Ga^{3+} for cobalt substitutions in the "114" compounds. In the following we report on polycrystalline samples synthesis, structural studies by X-ray diffraction and energy dispersive spectroscopy (EDS) coupled to electron diffraction, titration of the oxygen contents by iodometry, resistivity, Seebeck and magnetic susceptibility measurements for three series of $YBaCo_{4-x}M_xO_7$ compounds for $M = Al^{3+}$, Ga^{3+} and Zn^{2+} and small x values ($x \leqslant 0.4$). A very clear difference on the electronic properties is found to be induced by divalent or trivalent substituted cations even for amounts equal to 2.5% of foreign cation.

2. Experimental

The "114" compounds $YBaCo_{4-x}M_xO_7$ have been prepared by mixing precursors Y_2O_3 (dried at 900 °C) from Aldrich (99.99), $BaCO_3$ (Aldrich 99.999), Co_3O_4 (Normapur 99.9) and M_2O_3 ($M = Ga^{3+}$, Al^{3+}) or ZnO according to the "114" stoichiometric cation ratio with x values up to $x = 2$, 1 and 1 for $M = Ga^{3+}$, Al^{3+}

* Corresponding author. Fax: +33 2 31 95 16 00.
E-mail address: antoine.maignan@ensicaen.fr (A. Maignan).

0022-4596/$ - see front matter © 2008 Elsevier Inc. All rights reserved.
doi:10.1016/j.jssc.2008.02.031

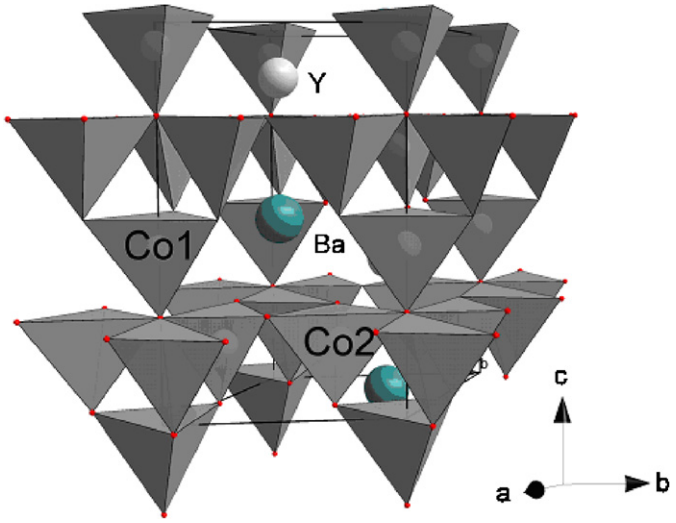

Fig. 1. Drawing of the structural $YBaCo_4O_7$ model showing along $\vec{c}$ the alternating CoO_4 tetrahedra layers, triangular (Co1) and Kagomé (Co2). Ba^{2+} and Y^{3+} are represented by the larger and medium size spheres, respectively.

and Zn^{2+}, respectively. The precursor was first heated at 900 °C for 24 h for decarbonation. For the sintering step, the samples were prepared in bar shapes ($2\times2\times10$ mm) by pressing the powders. They were then heated at 1200 °C for 48 h and then quenched in air at room temperature. The structure of the obtained black powders was systematically checked by X-ray powder diffraction "XRPD" data which were collected by using a Panalytical X-pert Pro diffractometer (Cu $K\alpha$, $5^\circ\leqslant2\theta\leqslant120^\circ$) equipped with a X'celerator detector. For the larger contents of substituting cations, several additional grindings and post-treatments at 1200 °C were not found to improve the solubility limit. The study by transmission electron microscopy was performed with a JEOL 2011 FEG transmission electron microscope with an EDS analyzer. Oxygen contents of the samples were estimated by iodometric titration [15]. The resistivity (ρ) measurements were made by the four-probe technique using ultrasonically deposited indium contacts. The T dependent ρ data were collected by using a Quantum Design physical properties measurement system (PPMS). A steady-state technique was used in the same set-up in order to measure the Seebeck coefficient (S) with a typical gradient of $\Delta T=1$ K [16]. The ρ and S data were performed upon cooling from 400 to 315 K, respectively. Magnetic susceptibility was obtained by dividing the magnetization (M) by the magnetic field (0.3 T) with M data collected in zero-field-cooling mode with a SQUID magnetometer (MPMS, Quantum Design).

3. Structural features

The solubility limits were first determined by EDS analysis starting from compositions with large substitution amounts ($x\geqslant1$). Since this technique is coupled to electron diffraction, this allowed to select the microcrystals having the expected unit cell for the "114" structure. By doing so, for the synthesis conditions aforementioned, the analyzed largest fractions of substituting cations are $x\sim0.3$, ~0.2 and ~1.2 for $M=Zn^{2+}$, Al^{3+} and Ga^{3+}, respectively. For instance, starting from the nominal composition "$YBaCo_{2.5}Ga_{1.5}O_x$", the average Ga^{3+} content in the microcrystals corresponds to the cation composition "$Y_{1.09}Ba_{0.78}Co_{2.87}Ga_{1.26}$". In that case, the gallium and barium deficiencies were found to correspond to an impurity with a 1:2 ratio for Ba:Ga. In order to compare substituted compounds with rather similar range of M contents, the structural study from XRPD data was limited to compounds with nominal compositions such as $x\leqslant0.4$, except for $M=Al^{3+}$ which solubility is the smallest. An example of partial solid solution is illustrated by the diffraction patterns in Fig. 2a for the Ga^{3+} substituted series. To measure the evolution of the unit cell parameters with x, the XRPD patterns collected at room temperature were refined in the orthorhombic $Pbn2_1$ space group [7] previously used to refine the pristine $YBaCo_4O_7$ compound (unit cell volume Table 1). For the unsubstituted $YBaCo_4O_7$, the better reliability factors of the refinements in this space group rather than in a trigonal space group was explained in Ref. [3] by the structural transition temperature which is beyond room temperature ($\sim$310 K). However, a clear change in the cell parameters evolution is found as x increases with a tendency towards the trigonal symmetry. As shown in the inset of Fig. 2b, this symmetry change to $P31c$ space group makes the peak indicated by an arrow disappearing as one goes from $x=0.0$ to 0.3. This symmetry change is also confirmed by the difficulty to choose between the two space groups for the $x=0.1$ compositions ($M=Zn^{2+}$, Ga^{3+}). Consequently, for all the substituted compounds the trigonal metric was used (Table 1) together with values calculated within the $Pbn2_1$ orthorhombic space group in order to compare the unit cell volumes to the pristine phase.

An example of the comparison for experimental and calculated ($P31c$ space group) diffraction patterns of $YBaCo_{3.7}Ga_{0.3}O_7$ ($x=0.3$) is given in Fig. 2b. The corresponding structural reliability factors listed in Table 2 attest for the quality of the structural refinements.

The change of symmetry for the substituted compounds suggests that the structural transition $Pbn2_1\rightarrow P31c$, observed for the pristine compound above room temperature ($T_S\sim310$ K), is either suppressed or that its characteristic temperature T_S has been shifted below room temperature. From the inspection of the data in Table 1, the following remarks can be made:

- The cell volume evolution with x is contrasted for the trivalent cations: it increases or decreases for Ga^{3+} ($r_{IV}=0.047$ nm) and Al^{3+} ($r_{IV}=0.039$ nm), respectively. Since both ionic radii are smaller than high spin Co^{2+} ionic radius ($r_{IV}=0.058$ nm), this strongly suggests that these cations are substituted for Co^{3+}.
- Interestingly, for the divalent Zn^{2+} substitution, the volume changes are intermediate between those measured for Al^{3+} and Ga^{3+}. Since Zn^{2+} ionic radius is the largest ($r_{IV}=0.060$ nm), this strongly suggests that the substitution occurs at the Co^{2+} site of similar ionic radius ($r_{IV}=0.058$ nm) so that it does not affect too much the unit cell volume.

The other important parameter in Table 1 concerns the oxygen contents which values do not show any clear trend depending on the substituted cation. These values are rather constant which supports that all the oxygen contents are close to the "O_7" oxygen stoichiometry. This implies that the mean cobalt oxidation state decreases as the content of substituting trivalent cation increases as shown for $M=Ga^{3+}$ in Table 1. From these rather constant values of oxygen content, the disordering effect upon the triangular frustration, induced by an oxygen uptake due to the substitution, as recently shown in Ref. [17] for an $O_{8.1}$ "114" compound, cannot be considered.

4. Physical properties

The resistivity (ρ) data vs temperature for the three series of $YBaCo_{4-x}M_xO_7$ are given in Fig. 3. For divalent and trivalent foreign cations, a very distinct behavior is observed. On the one hand, it is remarkable that for only $x=0.1$ of trivalent cation, Ga^{3+} of Al^{3+}, i.e. 2.5% of substituting cations per cobalt, the transition

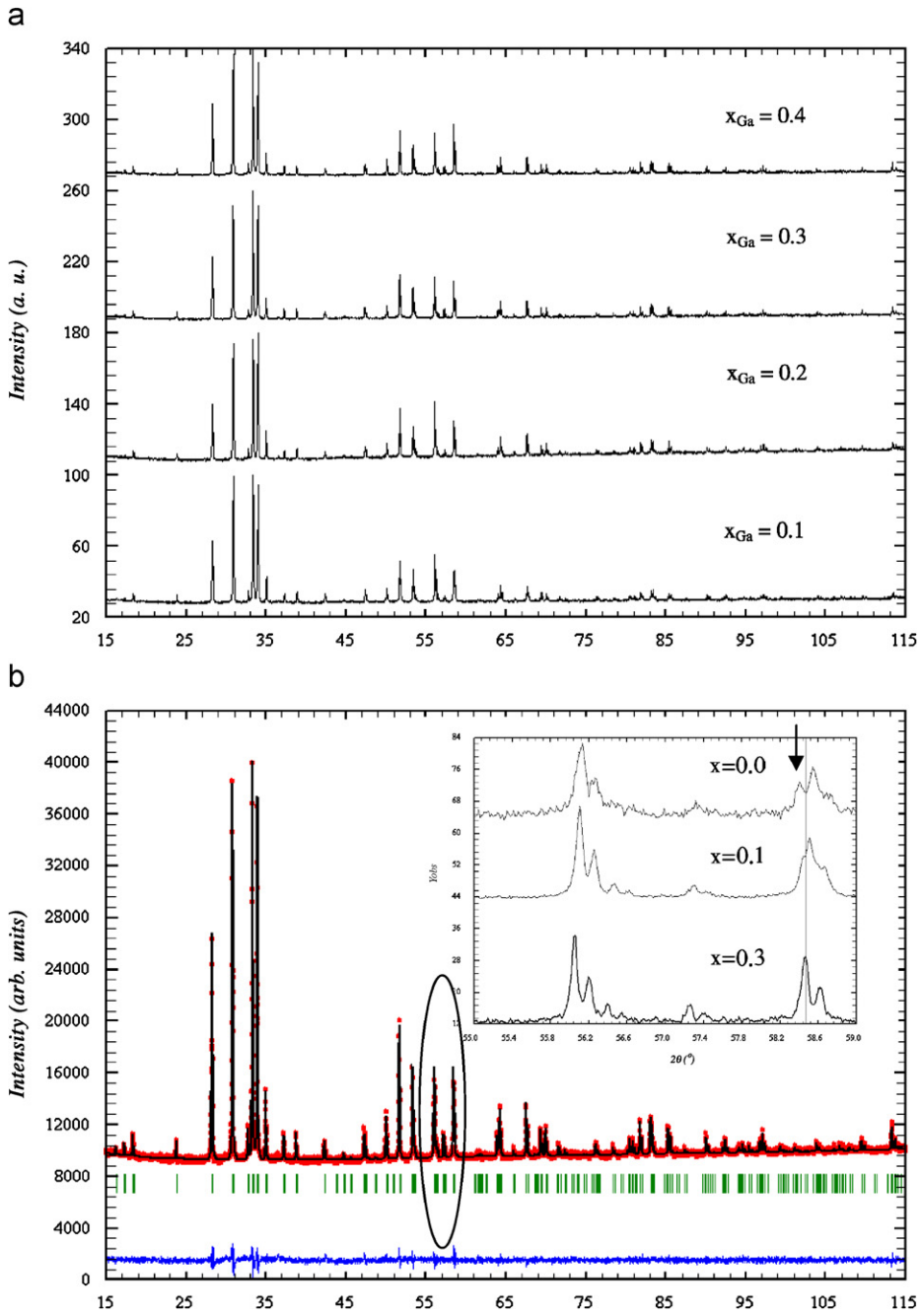

Fig. 2. Experimental powder X-ray diffraction patterns related to the $YBaCo_{4-x}Ga_xO_7$ series from $x = 0.1$ to 0.4 (a) and Rietveld pattern for $YBaCo_{3.7}Ga_{0.3}O_{6.99}$ ($x = 0.3$) (b). For the latter, the difference between experimental and calculated diffraction patterns is given as a bottom line. The row of markers indicates the positions of allowed reflections for space group $P31c$. The circled part is enlarged as an inset to show that the $Pbn2_1$ ($x = 0$) symmetry, with a characteristic peak indicated by the arrow, evolves to $P31c$ ($x = 0.3$).

located at T_S~310 K is suppressed (Fig. 3a and b for $M = Ga^{3+}$ and Al^{3+}, respectively). This goes together with a resistivity upward shift as x increasing, i.e., as these foreign cations act as scattering centers. This suppression of the electrical transition is also confirmed by the disappearance of the change of slope observed at T_S on the reciprocal magnetic susceptibility curves [$\chi^{-1}(T)$] shown in Fig. 4 for $x = 0.2$: for both $M = Ga^{3+}$ and Al^{3+}, the transition at T_S~310 K is suppressed as compared to the undoped $YBaCo_4O_7$ sample.

This behavior induced by trivalent cations is in marked contrast with the effect of the divalent cation. As shown in Fig. 3c, the signature of the transition on the $\rho(T)$ curves remains up to $x = 0.3$ in $YBaCo_{4-x}Zn_xO_7$ and, interestingly, this transition temperature decreases from 310 K for $x = 0$ to 260 K for $x = 0.3$. This trend is confirmed by the $\chi^{-1}(T)$ curves of the $x = 0$ and 0.3 "Zn" substituted "114" compounds in the inset of Fig. 4, showing that the transition is at a lower T_S value for the latter. A study of the Zn^{2+}-substituted 114 phase was already reported but for larger Zn^{2+} concentration starting from $YBaCo_{3.5}Zn_{0.5}O_{7-\delta}$, [18], i.e. for Zn^{2+} contents where our compounds were not found to be pure.

In order to confirm the difference between divalent and trivalent cations, Seebeck (S) measurements, which have been shown to be very sensitive to the structural transition [6], have been also made for selected compounds. As shown in Fig. 5, the S values taken upon cooling for the pristine compound $YBaCo_4O_7$, show an abrupt jump close to T_S with $S(T)$ values varying from an

Table 1
Unit cell parameters and volume at room temperature, oxygen content values ($7-\delta$) from titrations (taking into account the nominal formulas) and corresponding cobalt average oxidation state of cobalt (v_{Co}) for the series $YBaCo_{4-x}M_xO_{7-\delta}$

M	x nominal value	a (Å)	b (Å)	c (Å)	v (Å^3)	$7-\delta$ (± 0.02)	v_{Co}
$Co^{2+/3+}$	0.0	6.298	10.939	10.228	704.646	0.00	2.25
Zn^{2+} (0.60 Å)	0.1	6.297	10.943	10.231	705.018	7.03	2.27
		6.307		10.231			
	0.2	6.2987	10.9439	10.2339	705.447	7.07	2.33
		6.307		10.2339			
	0.4	6.3007	10.912	10.268	705.997	7.05	2.29
		6.307		10.268			
Ga^{3+} (0.47 Å)	0.1	6.302	10.932	10.235	705.049	6.99	2.23
		6.306		10.235			
	0.2	6.308	10.926	10.241	705.828	6.97	2.19
		6.308		10.241			
	0.3	6.309	10.928	10.246	706.469	6.99	2.18
		6.309		10.246			
	0.4	6.3090	10.9275	10.249	706.579	6.98	2.15
		6.309		10.249			
Al^{3+} (0.39 Å)	0.1	6.300	10.9122	10.226	703.050	6.97	2.22
		6.300		10.226			
	0.2	6.295	10.903	10.228	702.014	7.00	2.21
		6.295		10.228			

All the unit cell volumes are given keeping an orthorhombic space group $Pbn2_1$. For the substituted samples, the corresponding unit cell parameters in the $P31c$ ($a = b$) space group are also given in a second line. The ionic radius values of the substituted M cations are indicated in brackets.

Table 2
Structural parameters from Rietveld refinements for $YBaCo_{3.7}Ga_{0.3}O_{7.00}$

Atomic parameters								
Atom	Ox.	Wyck.	Site	S.O.F.	x/a	y/b	z/c	U (Å^2)
Y	+3	2*b*	3*m*		2/3	1/3	0.9318(3)	0.0030
Ba	+2	2*b*	3*m*	1.002	2/3	1/3	0.5599(1)	0.0227
Co1	+3	2*a*	3*m*	1.014	0	0	0.4853(5)	0.0001
Co2	+2	6*c*	*m*	0.979	0.1719(2)	0.8275(5)	0.7494(7)	0.0038
O1	−2	6*c*	*m*	0.971	0.5313(5)	0.5314(7)	0.8079(4)	0.0050
O2	−2	2*a*	3*m*	0.928	0	0	0.3181(3)	0.0124
O3	−2	6*c*	*m*	1.096	0.2019(3)	0.8754(6)	0.539(1)	0.0062
Space-group		*P*31*c* (159)—trigonal						
Cell		$c = 10.2460(2)$ Å				$\chi^2 = 2.27$		
		$a = 6.3095(1)$ Å				$R_B = 6.42\%$		
		$c/a = 1.6239$				$R_F = 9.43\%$		
		$V = 353.24$ Å^3						

almost T-independent value of $S = 150\,\mu V\,K^{-1}$ beyond T_S to values that increase as T decreases below T_S from $170\,\mu V\,K^{-1}$ at 290 K to $210\,\mu V\,K^{-1}$ at 100 K. For the Zn^{2+} substituted compounds, in agreement with the T_S decrease indirectly observed from the $\rho(T)$ and $\chi^{-1}(T)$ curves, the $S(T)$ curves reveal also an abrupt jump with decreasing T_S values as the Zn^{2+} content (x) increases as shown for $x = 0.2$ and 0.3 in Fig. 5a. This T_S evolution is also accompanied by a decrease of the S values beyond T_S as x increases.

As previously reported [6], for $T \gg T_S$, the S values can be explained by using the Heikes formula,

$$S = -\frac{k_B}{e}\ln\left(\beta\frac{y}{1-y}\right), \quad (1)$$

with y the "Co^{3+}" hole fraction over all cobalt sites and β the spin degeneracy term $\beta = (2S+1)^{Co^{2+}}/(2S+1)^{Co^{3+}}$. The best fitting to the data was obtained by considering a mixture of high-spin Co^{2+} and Co^{3+} with the corresponding e_g and t_{2g} orbitals splitting for the tetrahedral coordination leading to $\beta = 4/5$. Since for $T > T_S$, S decreases as x increases, it turns out that y, i.e. the "Co^{3+}" hole fraction, increases. This gives further support to the assumption that Zn^{2+} mainly substitutes for Co^{2+} which makes the $y = Co^{3+}/(Co^{2+}+Co^{3+})$ ratio increases.

On the opposite, the substitutions by trivalent cations suppress the transition on the $S(T)$ curves as shown for the Al^{3+}- and Ga^{3+}-substituted compounds in Fig. 5b and c, respectively. In contrast to the effect of the Zn^{2+} substitution, at high T, S increases with x for Al^{3+} and Ga^{3+}. This strongly supports that the Co^{3+} "holes" content decreases, i.e., Ga^{3+} or Al^{3+} substitutes principally for Co^{3+} cations. At that point, according to Eq. (1), it must be emphasized that the S changes at 300 K from $175\,\mu V\,K^{-1}$ ($M = Ga^{3+}$, $x = 0.2$) to $140\,\mu V\,K^{-1}$ ($M = Zn^{2+}$, $x = 0.2$) would formally correspond to an increase of the cobalt mean oxidation state from $v_{Co} = 2.14$ to 2.20. Though these absolute values differ from those deduced from iodometric titrations (Table 1), this $\Delta v_{Co} = 0.06$ decrease is consistent with the trend observed in the Ga^{3+}-substituted series (Table 1). In that respect, the Seebeck appears to be more sensitive than the titrations in the Zn^{2+}-series: although the oxygen content values are all in the estimated error of the technique, the change from $S = 150\,\mu V\,K^{-1}$ for $x = 0$ to $S = 140\,\mu V\,K^{-1}$ for $x = 0.2$ in the $YBaCo_{4-x}Zn_xO_{7-\delta}$ series would correspond to a Δv_{Co} increase of +0.018.

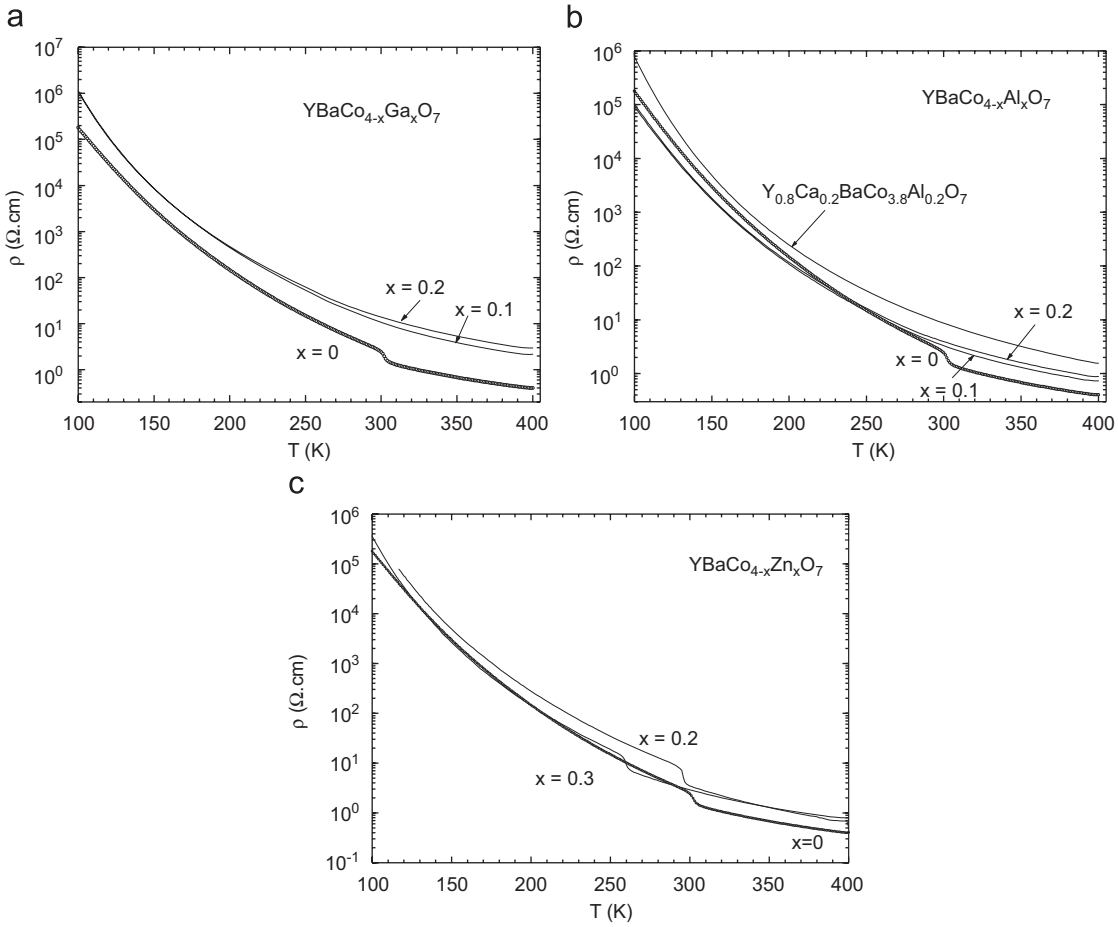

Fig. 3. *T*-dependent resistivity (ρ) for $YBaCo_{4-x}M_xO_7$ with $M = Ga^{3+}$ (a), $M = Al^{3+}$ (b) and $M = Zn^{2+}$ (c). The curve for $Y_{0.8}Ca_{0.2}BaCo_{3.8}Al_{0.2}O_7$ is also given in (b).

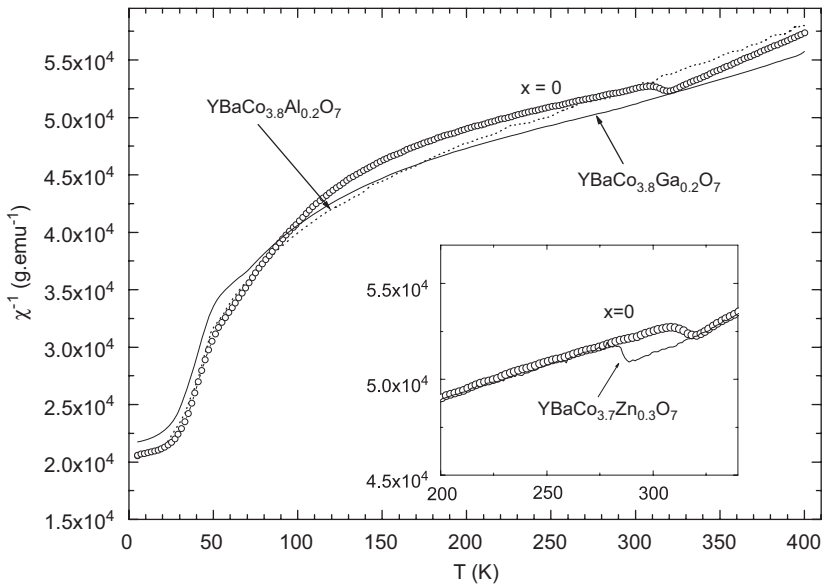

Fig. 4. *T*-dependent reciprocal magnetic susceptibility (χ^{-1}) of $YBaCoO_7$, $YBaCo_{3.8}Ga_{0.2}O_7$ and $YBaCo_{3.8}Al_{0.2}O_7$. Inset: $YBaCo_4O_7$ and $YBaCo_{3.7}Zn_{0.3}O_7$.

5. Discussion and concluding remarks

All the present experimental data point towards a very contrasted behavior between small amounts of divalent (Zn^{2+}) and trivalent (Ga^{3+}, Al^{3+}) cations substituted for cobalt in $YBaCo_4O_7$. Though the T_S decrease induced by Zn^{2+} is reminiscent of the T_S variation obtained by varying the rare-earth ionic radius r_L^{3+}, the effect of chemical pressure cannot be invoked: the Zn^{2+} substitution creates both slight unit cell expansion and T_S decrease, whereas the decrease of volume unit cell induced by decreasing r_{Ln3+} in $LnBaCo_4O_7$ makes T_S decreasing [9]. Furthermore, the S decrease as x increases in $YBaCo_{4-x}Zn_xO_7$, observed

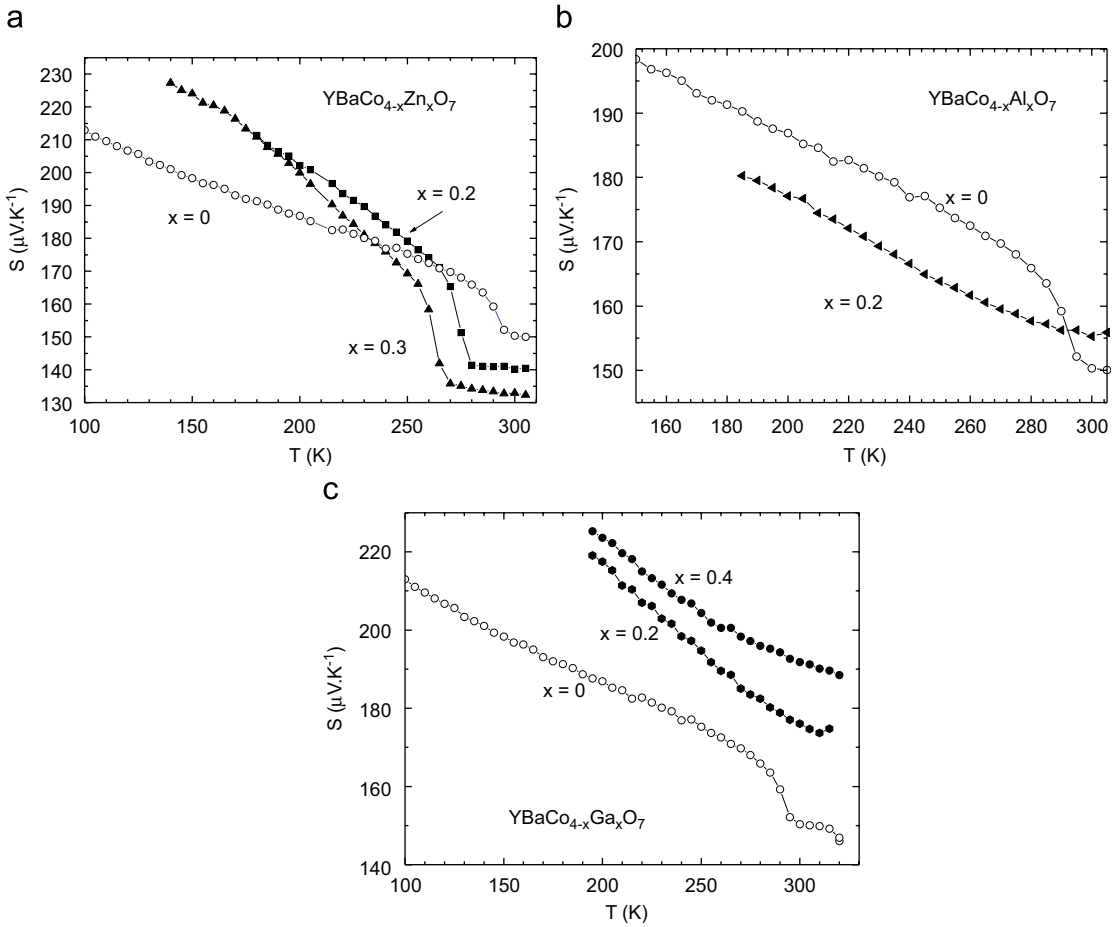

Fig. 5. *T*-dependent Seebeck (*S*) coefficient curves. (a) $YBaCo_{4-x}Zn_xO_7$, $x = 0$, $x = 0.2$ and $x = 0.3$; (b) $YBaCo_{4-x}Al_xO_7$, $x = 0$ and 0.2; (c) $YBaCo_{4-x}Ga_xO_7$, $x = 0$, 0.2 and 0.4.

beyond T_S, indicates an increase of the hole fraction. The situation differs from that observed for trivalent substitutions of Al^{3+} or Ga^{3+} for cobalt. First, Al^{3+} or Ga^{3+} make decreasing or increasing the unit cell volume, respectively, but for both cations a suppression of the structural transition is suggested by the physical properties. Clearly, the chemical pressure effect upon T_S invoked in the case of lanthanides (or Y^{3+}) does not explain the present result. However, the lower cobalt oxidation states, obtained by chemical titration in the case of Ga^{3+} substitutions as the amount of this trivalent cation increases, is consistent with the *S* increase found for Al^{3+} and Ga^{3+}.

This first analysis of the present experimental data strongly suggests that the main effect of the cation substitution is related to the changes of the cobalt oxidation states. This would rule out a scenario based on the site selectivity, at the Co(1) or Co(2) sites, of the substitution with a destabilizing effect of a $3Co^{2+}$:$1Co^{3+}$ charge ordering at the Kagomé [Co(2)] and triangular [Co(1)] sites, respectively. In order to check further the site selectivity of the substitution, a calcium-aluminium co-substituted sample, $Y_{0.8}Ca_{0.2}BaCo_{3.8}Al_{0.2}O_7$, was also prepared. A total substitution of Y^{3+} by heterovalent Ca^{2+} was reported to be possible in $YBaCo_4O_7$ [2]. For $Y_{0.8}Ca_{0.2}BaCo_{3.8}Al_{0.2}O_7$, the co-substitution is expected to compensate the charge effect of the Al^{3+} substitution on the cobalt oxidation state (v_{Co}). This is confirmed by the titration yielding $v_{Co} = 2.27$ and correspondingly an oxygen content $O_{7.01}$. This value is rather similar to the values obtained for the zinc-substituted compounds. Nevertheless, as shown by its resistivity curve $\rho(T)$ in Fig. 3b, the transition signature has also disappeared for $Y_{0.8}Ca_{0.2}BaCo_{3.8}Al_{0.2}O_7$. Thus, it is difficult to invoke subtle changes of the oxygen content. One alternative explanation to the oxygen content changes could be the crystallographic site selectivity of these substitutions, with an affinity of the trivalent cations for Co(1) (triangular layer) against a preferential Zn^{2+} location at the Co(2) (Kagomé layer). Considering that the Co(1) tetrahedra are connecting two successive Kagomé planes of Co(2), the preferential occupation of the former by the substituted trivalent impurity would rapidly limit the charge hopping between the Kagomé planes as if the electronic conductivity would evolve from 3D to 2D. This would make increasing the electrical resistivity and also rapidly hindering the structural transition by destabilizing the $3Co^{2+}$:$1Co^{3+}$ charge ordering.

References

[1] M. Valldor, M. Anderson, Solid State Sci. 4 (2002) 923.
[2] M. Valldor, Solid State Sci. 6 (2004) 251.
[3] A. Huq, J.F. Mitchell, H. Zheng, L.C. Chapon, P.G. Radaelli, K.S. Knight, P.W. Stephens, J. Solid State Chem. 179 (2006) 1125.
[4] L.C. Chapon, P.G. Radaelli, H. Zheng, J.F. Mitchell, Phys. Rev. B 74 (2006) 172401.
[5] M. Valldor, Solid State Sci. 7 (2005) 1163.
[6] A. Maignan, V. Caignaert, D. Pelloquin, S. Hébert, V. Pralong, J. Hejtmanek, D. Khomskii, Phys. Rev. B 74 (2006) 165110.
[7] V. Caignaert, A. Maignan, V. Pralong, S. Hébert, D. Pelloquin, Solid State Sci. 8 (2006) 1160.
[8] M. Karppinen, H. Yamauchi, S. Otami, T. Fujita, T. Motohashi, Y.H. Huang, M. Valkeapää, H. Fjellåg, Chem. Mater. 18 (2006) 490.
[9] N. Nakayama, T. Mizota, Y. Ueda, A.N. Sokolov, A.N. Vasiliev, J. Magn. Magn. Mater. 300 (2006) 98.
[10] W. Schweika, M. Valldor, P. Lemmens, Phys. Rev. Lett. 98 (2007) 067201.
[11] M. Soda, Y. Yasui, T. Moyoshi, M. Sato, N. Igawa, K. Kakurai, J. Phys. Soc. Jpn. 75 (2006) 054707.1.
[12] E.V. Tsipis, V.V. Kharton, J.R. Frade, Solid State Ion. 177 (2006) 1823.
[13] M. Valldor, J. Phys. Condens. Matter 16 (2004) 9209.
[14] M. Valldor, J. Phys. Chem. Solids 66 (2005) 1025.

[15] A. Maignan, S. Hébert, V. Caignaert, V. Pralong, D. Pelloquin, J. Solid State Chem. 178 (2005) 868.
[16] A. Maignan, C. Martin, M. Hervieu, B. Raveau, J. Hejtmanek, J. Appl. Phys. 89 (2001) 2232.
[17] O. Chmaissem, H. Zheng, A. Huq, P.W. Stephens, J.F. Mitchell, J. Solid State Chem. (2008).
[18] H. Hao, Z. Zhang, Q. He, C. Chen, X. Hu, Solid State Commun. 141 (2007) 191.